Atmos. Chem. Phys., 10, 8481–8498, 2010
www.atmos-chem-phys.net/10/8481/2010/
doi:10.5194/acp-10-8481-2010

Atmospheric Chemistry and Physics

Multi-annual changes of NO_x emissions in megacity regions: nonlinear trend analysis of satellite measurement based estimates

I. B. Konovalov[1,2], **M. Beekmann**[2], **A. Richter**[3], **J. P. Burrows**[3,4], **and A. Hilboll**[3]

[1]Institute of Applied Physics, Russian Academy of Sciences, Nizhniy Novgorod, Russia
[2]Laboratoire Inter-Universitaire de Systèmes Atmosphériques, CNRS, UMR 7583, Université Paris-Est and Université Paris 7, Créteil, France
[3]Institute of Environmental Physics and Remote Sensing, IUP/IFE, University of Bremen, Bremen, Germany
[4]Center for Ecology and Hydrology, Wallingford, UK

Received: 2 April 2010 – Published in Atmos. Chem. Phys. Discuss.: 23 April 2010
Revised: 26 August 2010 – Accepted: 6 September 2010 – Published: 8 September 2010

Abstract. Hazardous impact of air pollutant emissions from megacities on atmospheric composition on regional and global scales is currently an important issue in atmospheric research. However, the quantification of emissions and related effects is frequently a difficult task, especially in the case of developing countries, due to the lack of reliable data and information. This study examines possibilities to retrieve multi-annual NO_x emissions changes in megacity regions from satellite measurements of nitrogen dioxide and to quantify them in terms of linear and nonlinear trends. By combining the retrievals of the GOME and SCIAMACHY satellite instrument data with simulations performed by the CHIMERE chemistry transport model, we obtain the time series of NO_x emission estimates for the 12 largest urban agglomerations in Europe and the Middle East in the period from 1996 to 2008. We employ then a novel method allowing estimation of a nonlinear trend in a noisy time series of an observed variable. The method is based on the probabilistic approach and the use of artificial neural networks; it does not involve any quantitative a priori assumptions. As a result, statistically significant nonlinearities in the estimated NO_x emission trends are detected in 5 megacities (Bagdad, Madrid, Milan, Moscow and Paris). Statistically significant upward linear trends are detected in Istanbul and Tehran, while downward linear trends are revealed in Berlin, London and the Ruhr agglomeration. The presence of nonlinearities in NO_x emission changes in Milan, Paris and Madrid is confirmed by comparison of simulated NO_x concentrations with independent air quality monitoring data. A good quantitative agreement between the linear trends in the simulated and measured near surface NO_x concentrations is found in London.

Correspondence to: I. B. Konovalov
(konov@appl.sci-nnov.ru)

1 Introduction

The largest urban agglomerations (megacities) concentrating a considerable fraction of the world's population (see e.g. Brinkhoff, 2009) are known to be associated with serious air pollution problems and to contribute significantly to the global anthropogenic sources of air pollution (Molina and Molina, 2004; Marshall, 2005; Lawrence et al., 2007; Butler et al., 2008; Chan and Yao, 2008). The physical and chemical processes in the atmosphere of megacities and surrounding regions have been in the focus of numerous studies (see, e.g. Wang et al., 2006; de Foy et al., 2007; Molina et al., 2007; Lei et al., 2008; Miyakawa et al., 2008; Nunnermacker, et al., 2008; Esposito et al., 2009; Singh et al., 2009). To properly simulate these processes and to estimate the effects of air pollutant emissions in megacities on both local air quality and composition of the atmosphere on regional and global scales, atmospheric models should be provided with accurate information on emissions of air pollutants and their temporal variability. However, available estimates of air pollutant emissions in megacities are currently rather uncertain; this is reflected, specifically, in big differences between data of different "bottom-up" emission inventories (Butler et al., 2008). It is also poorly known to what extent the available emission inventories are capable to reflect actual inter-annual and multi-annual changes in emission rates.

Published by Copernicus Publications on behalf of the European Geosciences Union.

As an alternative to the "bottom-up" emission inventory approach which requires detailed information about sources and emission factors, there is a possibility to derive emission estimates directly from ambient measurements (see, e.g., Enting, 2002). The "measurement-based" approach proved to be especially fruitful when used with satellite measurements of the composition of the troposphere. In particular, it has been demonstrated that satellite measurements of nitrogen dioxide can be used for identification of NO_x emission sources (Richter et al., 2004; Beirle et al., 2004; Jaeglé, et al., 2004; Beirle et al., 2006; Boersma et al., 2005; Martin et al., 2007; Lin et al., 2010), validation and improving of available data on the spatial structure of NO_x emissions (Martin et al., 2003, 2006; Konovalov et al., 2006a, b; Toenges-Schuller et al., 2006; Napelenok et al., 2008), as well as a source of independent information on their temporal variability (Beirle et al., 2003; Bertram et al., 2005; Wang et al., 2007; Boersma et al., 2008; Kaynak et al., 2009) and multi-annual changes (e.g., Richter et al., 2005; van der A et al., 2006, 2008; Uno et al., 2007; Konovalov et al., 2008; Stavrakou et al., 2008; Kim et al., 2009; Kurokawa et al., 2009) both on global and regional scales.

Here we discuss satellite measurement-based estimates of NO_x emission trends in several megacity regions in Europe and the Middle East. To our knowledge, the NO_x emission trends in the compact regions considered in this study have not yet been addressed in any dedicated study, although some relevant estimates have been reported in the framework of a more general global or continental-scale analysis (Konovalov, 2007; Konovalov et al., 2008; van der A et al., 2008). Note that some major urban agglomerations considered here do not satisfy the common definition of a megacity as a metropolitan area with a total population in excess of 10 million people, but, nevertheless, we refer to all these densely populated areas (having a total population of more than 4 million people) as megacities for the sake of conciseness. The method used here involves a simple combination of retrievals of GOME and SCIAMACHY satellite instrument data with model-simulated NO_2 columns. The satellite measurements of NO_2 columns are available since 1996; the period addressed in this study includes 13 years (1996–2008). Importantly, we do not assume that the estimated emission changes can be adequately described in terms of a linear trend. Although this assumption proved to be useful in previous papers analysing multi-annual changes in NO_2 columns measured by satellites (e.g., Richter et al., 2005; van der A et al., 2006, 2008; Konovalov et al., 2008), it appears to become less adequate as the analysed time series becomes longer. Unfortunately, while the linear trend analysis can be done with a standard technique, there exists no common methodology which could be employed to estimate nonlinear trends in any arbitrary case. One of the easiest ways to account for a possible nonlinearity of a trend is to fit the data by means of piece-wise linear regression models. This technique has been useful, in particular, in studies aimed at detection of a "turnaround" point in the trend of stratospheric ozone (see e.g., Reinsel et al., 2005; Vyushin et al., 2007). A more general approach to detect a nonlinear trend from a noisy time series of a measured characteristic is based on the spectral analysis (see, e.g. Moore et al., 2005 and references therein). However, the spectral analysis would not be helpful in our case because the available record of NO_2 columns retrieved from satellite measurements is too short.

Here we perform a nonlinear trend analysis by means of an original algorithm based on the probabilistic Bayesian approach which is common for inverse modelling and data assimilation studies. The basic ideas of our method are the use of artificial neural networks for approximating nonlinear trends and a cross validation technique for constraining the optimal fit and for estimation of random uncertainties in the input data. The applicability of the method is based on a few general assumptions, but it is not assumed that the trend has any specific character.

An important feature of our analysis is that it does not involve any subjectively-defined a priori quantitative constraints which are typically involved in inverse modelling studies. Another distinctive feature of this study is the use of independent multi-annual data of air quality monitoring in several megacities for validation of NO_x emission trends derived from satellite measurements. The comparison with surface measurements is important in view of possible systematic uncertainties in the derived trend estimates, which otherwise are difficult to evaluate.

The paper is organised as follows. The data used for our analysis are described in Sect. 2. The methods employed to derive time series of annual estimates of NO_x emissions in megacity regions from satellite measurements and to evaluate nonlinear trends in NO_x emissions are presented in Sect. 3. The results of our analysis and their validation are discussed in Sect. 4. Section 5 summarises the major findings of this study.

2 Measurement and model data

2.1 Satellite data

We use retrievals of the data of the GOME (Burrows et al., 1999) and SCIAMACHY (Bovensmann et al., 1999) instruments onboard the ERS-2 and ENVISAT-1 satellites of the European Space Agency (ESA). We employ seven years (1996–2002) of the GOME measurements combined with six years (2003–2008) of the SCIAMACHY measurements. The GOME measurements were performed with a horizontal resolution of $320\times40\,km^2$. The satellite overpass time was about 10:30 local standard time (LST), and global coverage was achieved within three days at the equator. The nominal horizontal resolution of SCIAMACHY is much higher ($60\times30\,km^2$) but at the expense of a longer period needed to

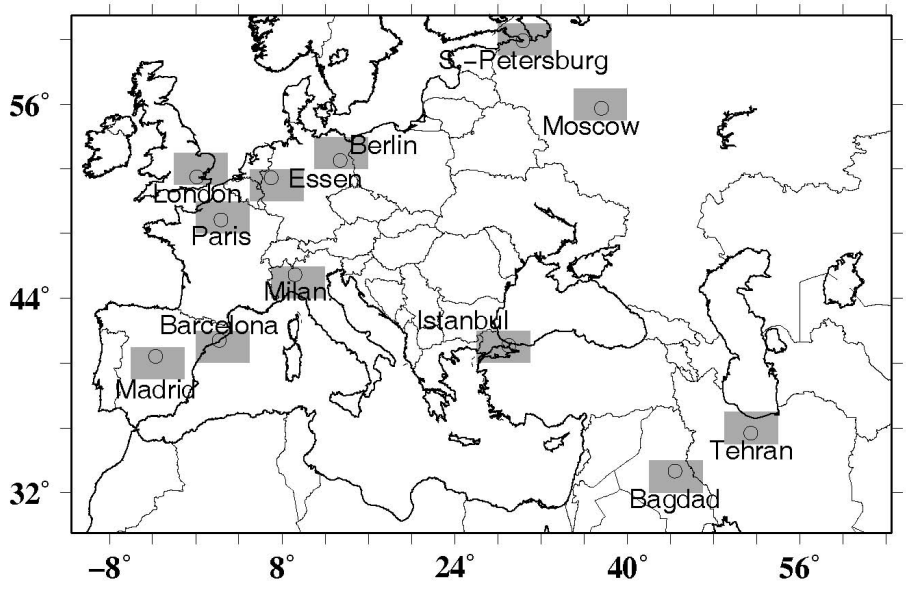

Fig. 1. The areas attributed in model simulations to the megacity regions considered in this study.

obtain full global coverage (6 days). The ENVISAT-1 overpass time is 10:00 LST at the equator.

The tropospheric NO_2 column data products used here have been retrieved from the satellite measurements by IUP, University of Bremen. The same data have already been used in several earlier studies (Richter et al., 2005; Kim et al., 2006, 2009; Konovalov et al., 2008). The general description of the retrieval procedure can be found in Richter et al. (2005) and Kim et al. (2009). Below we describe in detail only the data pre-processing stage specific for the given study.

The goal of the pre-processing stage is to get consistent time series of NO_2 columns for several areas selected for this study. Specifically, we consider the 12 largest urban agglomerations covered by the domain of our regional model in Europe and the Middle East. These agglomerations are marked in Fig. 1. Each of these agglomerations has a total population of more than 4 million. We do not consider the megacities of Cairo and Alexandria because they are situated too closely to be adequately addressed in our analysis. Initial daily data for tropospheric NO_2 columns were projected onto a $1^\circ \times 1^\circ$ grid and averaged over three summer months (June–August) of each year. To insure the consistency of the measurement data time series from the different instruments, the NO_2 column data from SCIAMACHY were convoluted over a typical area covered by the GOME measurements. The idea of this procedure is to simulate the smoothing of the spatial structure of NO_2 columns, introduced by the GOME measurement:

$$c^{\mathrm{conv}}_{s(i)} = \sum_{j=0}^{2m} c_{s(i-m+j)} \rho_j \left[\sum_{k=0}^{2\mathrm{m}} \rho_k \right]^{-1};$$

$$\rho_j = \exp\left(-\frac{[j-m]^2 \cos(\varphi)^2}{2 s_c^2} \right)^2 \quad (1)$$

where $c_{s(i)}$ are the original NO_2 column amounts in the grid cell i closest to a megacity centre, m is the number of grid cells on the longitudinal plane within 320 km (the typical resolution of the GOME measurements), φ is the latitude, and s_c is an effective distance scale. Such a transformation of the NO_2 columns is a heuristic method, which is used here because we had no more specific information about the relationship between the seasonally averaged NO_2 columns from GOME and SCIAMACHY. Note that the main complication in analytical consideration of this relationship is, specifically, due to the fact that the area covered by SCIAMACHY measurements is also, to some extent, smeared between several cells of our grid.

The value of the distance scale, s_c, was estimated to be equal 0.85 $\pm$0.16 (grid cells) by minimizing the mean squared difference between the convoluted NO_2 columns for 2003 and the original NO_2 columns (from GOME) for 2002 over the 12 megacities. Such an evaluation of s_c is made under the assumption that the change of NO_x emissions between the years 2002 and 2003 is small in comparison with the difference between the maximum and minimum NOx emission rates during the whole period of 13 years. The uncertainty of s_c is roughly estimated by repeating the same estimation of s_c independently for four randomly selected subsets of 3 different megacities and calculating the standard deviation of the obtained 4 independent estimates. This uncertainty is taken into account in our further analysis. Taking into account our estimate of s_c, the smoothing specified by Eq. (3) supposes (based on the analogy with properties of

the Gaussian distribution) that, for example, in the case of Paris, about 95 percent of the signal in the seasonally averaged GOME data comes from the actual NO_2 columns within 5 degrees of longitude or within about 360 km. Thus it should be kept in mind that we do not distinguish here between emissions in a given megacity and emissions in a surrounding urban agglomeration. The final steps of the pre-processing stage are the linear interpolation of the NO_2 columns between the two belts of grid cells closest to a megacity centre in the north-to-south direction and averaging of the interpolated data corresponding to these grid cells.

2.2 Data of ground-based measurements

In the context of the given study, the ground based measurements are an indispensable source of independent information on emission changes in the considered megacities. Specifically, the surface data are used for validation of the NO_x emission trends derived from satellite measurements. While several hundreds of NO_x monitors are currently operational in Europe, only few of them were continuously available during the whole period of 13 years considered, and not all of the monitoring data are publicly accessible. Here we used the available monitoring data for London, Madrid, Milan, and Paris.

The data for London agglomeration are obtained from (i) UK National Air Quality Archive (www.airquality.co.uk) and (ii) the London Air Quality Network (www.londonair.org.uk). The data for Madrid and Milan are taken from the Airbase database (http://air-climate.eionet.europa.eu/databases/airbase), and the data for Paris have been provided by AIRPARIF (http://www.airparif.asso.fr). The measurements are carried out by means of the chemiluminescence technique. In the cases of London and Paris, we were provided with NO_x ($NO+NO_2$) measurements for all summer seasons from 1996 to 2008. The available NO_x measurements in Madrid span the period of only 8 years (2000–2007), and only data of NO_2 measurements for the period from 1999 to 2007 were available for Milan. Note that even the limited records of measurements in Madrid and Milan were important to consider in view of interesting nonlinear features detected in our analysis (see Sect. 4.1).

To insure the consistency of the surface data with the satellite measurements, the raw hourly data (both from the model and measurements) have first been averaged over the period from 10:00 to 11:00 LST. Next, the daily data were processed to get the seasonally averaged (over three summer months) daily mean NO_x (or NO_2) concentrations. Taking into account that many days were not provided with data, some common criterion was needed for the selection of monitors. Here we chose to consider only those monitors that provided data for at least 60 days in each summer of the considered period. This criterion is a result of a subjective trade-off between quality and amount of the monitoring data. In view of the goal of our analysis, we opted to disregard measurements at traffic (or roadside) sites because of their low spatial representativeness: we took into account that the data from traffic monitors when combined with monitors of other types (e.g. with urban background monitors) could induce some disproportional biases in the estimated trend. However, as an exception we consider traffic monitors in Madrid because otherwise we would be left only with one monitor (of suburban industrial type). In total, we considered data from six monitoring sites in the London agglomeration, four sites in Madrid, six sites in Milan and ten sites in Paris. The selected sites are listed in Table 1.

2.3 Simulated data

In parallel with satellite data we use simulations performed with the CHIMERE chemistry transport model. CHIMERE is a three-dimensional Eulerian model designed to simulate air pollution in the boundary layer and free troposphere on the regional and continental scales. An in-detail description of CHIMERE is available on the web at http://www.lmd.polytechnique.fr/chimere/. The tropospheric NO_2 column amounts simulated by CHIMERE were evaluated against the SCIAMACHY and GOME measurements in earlier studies (Konovalov et al., 2005; Blond et al., 2007). In this study, the model's domain covers all of Europe, the Mediterranean and the Middle East with a horizontal resolution of $1^\circ \times 1^\circ$. This rather coarse resolution was chosen in view of computational costs of the study and also taking into account that the available multi-annual data of the EMEP emission inventory provided with the spatial resolution of $50 \times 50\,km^2$ did not allow us to increase the resolution of our simulations considerably using, e.g., a "nested domain" option. The simulations were performed with 12 vertical levels specified in hybrid coordinates with the top of the CHIMERE vertical domain fixed at 200 hPa pressure level. The multi-annual model runs are performed with constant boundary conditions specified by using monthly average ("climatological") values of the LMDZ-INCA2 model (Hauglustaine et al., 2004). Other specific features of the model configuration are the same as described in Konovalov et al. (2008). The simulated NO_2 columns were sampled consistently with the measurement-based daily NO_2 columns at the times of satellite overpasses. They were then averaged over three summer months and convoluted in the same way as the SCIAMACHY data (see Eq. 3).

CHIMERE was run independently for each summer season starting on 24 May with the same initial and boundary conditions. Anthropogenic emissions are based on the so-called "expert" annual data of the EMEP emission inventory (UNECE, 2009) for the years 1996–2007. The data were obtained from the EMEP web site on a $50 \times 50\,km^2$ grid in August 2009. As 2008 emission data were not available, they are filled in by a linear interpolation between years 2007 and 2010 (for the latter a "projection" was available). A base multi-annual run of CHIMERE was performed with constant NO_x emissions (corresponding to the year 2001),

Table 1. The air quality monitors selected for this study.

City	Monitor's name (location)	Monitor's type
London	London Bexley	suburban
	London N. Kensington	urban background
	London Elthem	urban background
	Rochester	rural
	Ealing-Town Hall	urban background
	Hackney-Clapton	urban background
Madrid	ES0116	urban traffic
	ES0117	urban traffic
	ES0123	urban traffic
	ES1162	industrial suburban
Milan	IT1017	suburban background
	IT1088	suburban background
	IT1174	rural background
	IT1203	suburban background
	IT0732	suburban background
	IT0774	rural background
Paris	Issy	urban
	Paris18	urban
	Paris12	urban
	Aubervilliers	urban
	Versailles	suburban
	Vitry	urban
	St.-Denis	urban
	Paris7	urban
	Montgeron	urban
	Bobigny	urban

while annual EMEP emission data are used for other species (NMVOC, CO and SO_x).

As an illustration of the CHIMERE performance, Fig. 2 shows the mean summertime values of NO_2 columns simulated by CHIMERE in comparison with corresponding values derived from SCIAMACHY measurements. The model tends, on the whole, to slightly underestimate the retrievals from satellite measurements, but such underestimation is not important for this study, because we consider variations of NO_2 columns in a relative scale. Stronger differences between the simulated and measured NO_2 columns in several Middle East countries and Spain are probably indicative of missing NO_x sources, as discussed in Konovalov et al. (2006a, b).

Taking into account the limited spatial resolution of the satellite data, the emission estimates for a given megacity are assumed to be representative of an area of $5^\circ \times 2^\circ$ (see Fig. 1). That is, the size of an urban agglomeration resolved in satellite measurements is assumed to be typically in the range from 200 to 300 km. Note that the NO_x emission trend estimates obtained in this study (see Sect. 4.1) do not depend in any way on this definition which is only used for interpretation and validation of our results.

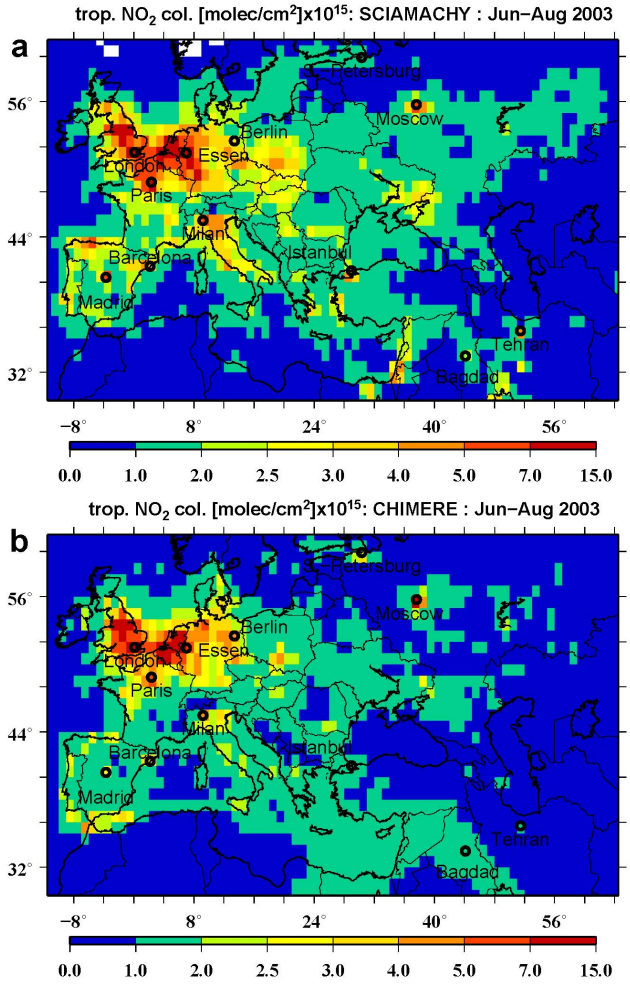

Fig. 2. Tropospheric NO_2 columns derived from SCIAMACHY measurements **(a)** in comparison with the corresponding NO_2 columns simulated by CHIMERE **(b)**. The data shown are averages over three summer months of 2003.

3 Method

3.1 Combining the measured and simulated NO_2 columns

We assume that the dependence of NO_2 columns on NO_x emissions can be approximated by a linear relationship:

$$C(t_i) \approx C_b(t_i) + \alpha(t_i) E(t_i) \quad (2)$$

where $C(t_i)$ is the seasonally averaged NO_2 column amount over a given megacity for a year i, $C_b(t)$ is the "background" NO_2 column amount which is not related to emissions from the given megacity, $E(t_i)$ is the seasonally averaged NO_x emission rate and $\alpha(t_i)$ is the sensitivity of the NO_2 columns to changes of the NO_x emissions, which is assumed to be independent on the NO_x emissions themselves. Having in

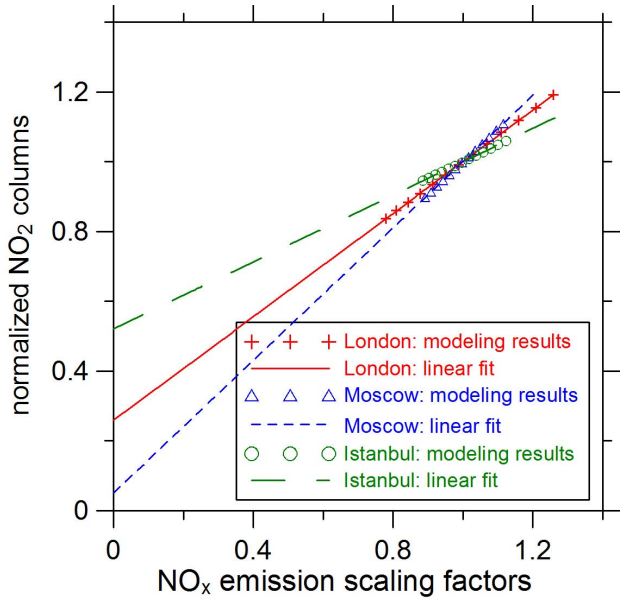

Fig. 3. A model-based test confirming the assumption about a linear dependence of NO_2 columns on NO_x emissions in megacity regions: the NO_x emission rates for the year 2001 have been scaled within the estimated range of NO_x emission changes in corresponding megacities from 1996 to 2008. The results are shown for three megacities (London, Moscow and Istanbul) representing different geographical regions. The intercept reflects the "background" NO_2 amounts which are not dependent on anthropogenic NO_x emissions in the considered megacities.

mind this linear approximation (2), we estimate the normalized annual emission rates as follows:

$$E(t_i)/E_0 \cong \frac{C_o(t_i) - C_{bm}(t_i)}{\gamma C_m(t_i)|_{E=E_0} - C_{bm}(t_i)} \quad (3)$$

where the indexes "o" and "m" denote the observed and modelled data, respectively, E_0 is the emission rate for the reference year (2001), and γ is the correction factor used to compensate for systematic differences between the simulated and observed NO_2 columns. The magnitude of γ is evaluated as the ratio C_o/C_m for the year 2001.

By employing the chemistry transport model in the context of Eq. (3) for inversion of the relation (2), we attempt to account for those variations in NO_2 columns that are due to meteorological variability and to estimate that part of the NO_2 columns over a megacity that is not associated with local anthropogenic NO_x emissions. It is particularly important to try to "filter-out" the changes in NO_2 columns associated with multi-annual meteorological variability such as, e.g., the North Atlantic Oscillation (see, e.g., Eckhardt et al., 2003). This approximation allows us to take into account also the changes in the NO_2 lifetime associated with the assumed changes of emissions of volatile organic compounds (VOC). The background NO_2 column amounts, $C_{bm}(t)$, were evaluated in a special model run with zero anthropogenic NO_x emissions. The changes in biogenic emissions are disregarded; as it was argued in Konovalov et al. (2008), they are much slower (at least in Europe) than changes in anthropogenic emissions. The contribution of anthropogenic emissions outside of a given agglomeration to NO_2 columns over the agglomeration is neglected.

Validity of the linear approximation in Eq. (2) was confirmed by a model test run which yielded an almost perfect linear relationship between NO_x emissions scaled in the range typical for the trends retrieved in this study and NO_2 columns calculated for all of the megacities considered (see Fig. 3). Another model run was performed to estimate the contribution of anthropogenic NO_x emissions outside of a given agglomeration to NO_2 columns over the agglomeration. In this run, the anthropogenic emissions in the megacity regions specified in Fig. 1 were put to zero. As a result, it has been estimated that the "external" part of NO_2 columns over the megacities is typically less than 15 percent. A corresponding bias in the estimated emission trend in a megacity depends on the trends in NO_x emissions in the surrounding regions. If the emission changes are similar in both the megacity and surrounding regions, then the effect of the external part of the NO_2 column amount should be rather negligible. In fact, both the EMEP emission inventory (Vestreng et al., 2009) and inverse modeling results (Konovalov et al., 2008) suggest there are no strong differences in NO_x emission changes between most of the regions considered here and their surroundings. A check of the self-consistency of our estimates for all the megacities regions has been performed: that is, the linear emission trend estimates obtained in this study were employed in the model to simulate NO_2 columns which were then used as input data in Eq. (3) instead of the satellite data, and the linear trends in the simulated NO_2 columns were compared with the linear trends in the original data from satellites. This test yielded an expected positive result, the difference between the linear trends in the measured and simulated NO_2 columns also being, on average, about 15 percent.

Note that the inter-annual variations of NO_x emissions ($E(t_i)/E_0$) can, in principle, be estimated directly from the measured NO_2 columns as the $C(t_i)/C_0$ ratio, where C_0 is the NO_2 columns in the reference year. Figure 4, where the relative variations of the measured NO_2 columns are shown on the same scale as variations of the NO_x emission estimates, gives an idea about the differences between the two approaches, and it also shows other quantities involved in Eq. (3). It can be seen that the difference in the temporal evolution of the measured NO_2 columns and the emission estimates is not large on average, but can be significant in some cases. In particular, the magnitudes of the linear trends in NO_x emissions are considerably larger than those in NO_2 columns in several Western European megacities (Berlin, London, Milan and Paris), and also in Bagdad, Tehran and Moscow. The impact of the background NO_2 columns on the estimates of NO_x emission trends is rather negligible in

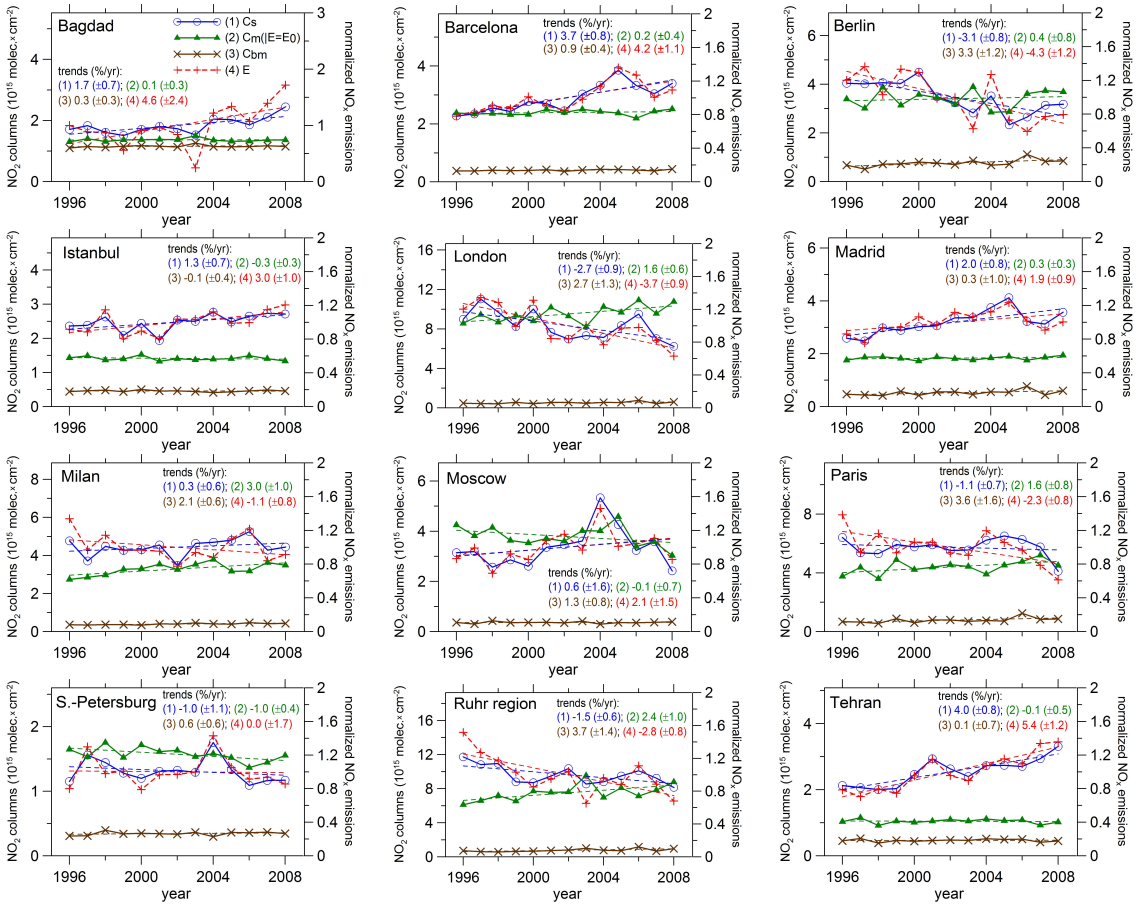

Fig. 4. The combined time series of satellite data $(1-C_s)$ for tropospheric NO_2 columns in comparison with the NO_2 columns simulated by CHIMERE with constant NO_x emissions $(2-C_m)$ and with zero anthropogenic emissions $(3-C_{bm})$. The time series of NO_x emission estimates $(4-E)$ are also shown. Magnitudes of slopes of linear fits are related to values of corresponding characteristics in 1996. Uncertainty range is given in terms of the 68.3 percentile (one sigma).

the cases of London and the Ruhr region (more specifically, if this impact were disregarded, then the resulting change in the linear NO_x emission trends would be less than 10 percent of their values) and the difference is mainly due to the trends in the modelled NO_2 columns (see C_m in Eq. 3). In contrast, the role of the background NO_2 columns is dominant in the cases of Bagdad and Tehran. In the other cases, the contributions of all factors to the differences between the trends in NO_x emission estimates and in measured NO_2 columns are about equally important. Additional analysis has revealed that the trends in the simulated data are mainly due to changes in emissions of volatile organic compounds (VOC). Specifically, the model shows that a decrease of VOC emissions (which, according to the EMEP inventory, took place in Western Europe during the considered period) is associated mainly with an increase of tropospheric NO_2 (presumably due to a decrease in OH concentration). Note, however, that the effect of VOC emission changes alone does not explain positive trends of the background NO_2 column amount simulated in megacities of France, Germany and Great Britain: there is also a contribution of long-term meteorological variability, but it remains unknown whether or not such variability is reproduced in our simulations adequately. In any case, the impact of trends in the background NO_2 columns on our results is quite negligible.

The fact that the inter-annual variations in the measured NO_2 columns are rather poorly reproduced by the model can be explained by considerable uncertainties in both the measured and simulated NO_2 columns. Taking into account that the uncertainty range of the linear trends (see Fig. 4) is larger in the case of the satellite data than in the cases of simulations in 8 out of 12 regions, it can be concluded that the random fluctuations in the measured NO_2 columns are larger than those in the simulations. However, this observation does not necessarily mean that the satellite data are more uncertain. Values of the simulated and measured NO_2 columns are in a rather good agreement in the reference year (2001) in most cities, except for Istanbul, Madrid, and

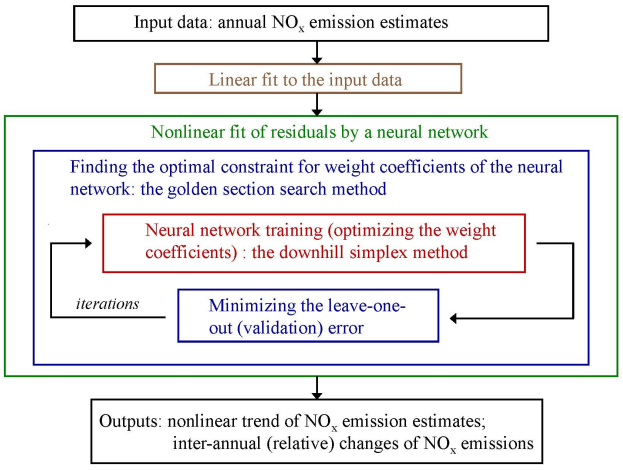

Fig. 5. Flow chart illustrating major steps of the algorithm for estimation of a nonlinear trend in a NO_x emission time series.

Tehran, where the simulated NO_2 columns are much lower than the measurement-based ones probably due to strongly underestimated NO_x emission rates (Konovalov et al., 2006a, b).

If the chemistry transport model were perfect, the inverse modelling approach employed in this study would definitely lead to more accurate results than the direct approach. This is the main reason for our choice. It should be kept in mind, however, that the estimates obtained by the inverse modelling may be affected by possible unspecified model errors, and that the "direct" method (used, for example, by Richter et al., 2005, van der A et al., 2008; Kim et al., 2009) can also enable a reasonable estimate of the NO_x emission trends in large urban agglomerations. In a general case, both approaches can be subject to some systematic errors which are difficult to estimate (otherwise they could be corrected). The detailed analysis of the differences between these two approaches goes beyond the scope of this paper.

The natural logarithms, $\boldsymbol{e}(=\ln(\boldsymbol{E}))$, of the estimates defined by Eq. (3) are used as input data for our analysis. A linear fit of these data gives an exponential fit for the emissions E, which optimally approximates the evolution of the emissions, assuming a constant relative rate of their inter-annual changes.

3.2 Estimation of a nonlinear trend

3.2.1 Formulation of the general problem

The estimation of the nonlinear trend in NO_x emission times series is a particular case of a general problem of estimation of a nonlinear trend of a natural characteristic x, by a noisy time series of its measurements (or estimates), y:

$$y_i = x_i + \varepsilon_i, i \in I_d \quad (4)$$

where i is the temporal index (e.g. the year number), ε are errors, and I_d ={1,..., n}. In our case, y are the natural logarithms of emission estimates obtained from Eq. (3). Let us make three simple assumptions, which seem to be reasonable in the considered situation. First, the noise is uncorrelated (white), so that $<\varepsilon_i \varepsilon_j>=0$ for any $i \neq j$, and $<\varepsilon_i^2>=\sigma^2$, where the angled brackets denote averaging over a statistical ensemble. Second, ε satisfies the normal distribution. And third, the changes of the real value x are smooth in comparison with the level of noise $(x_{i+1}-2x_i+x_{i-1})^2 \ll \sigma^2$ for any i. This condition implies that we can disregard any single measurement without losing essential (available) information about the trend.

Our goal is to obtain a series of estimated values x_e, such that $(x_{ei}-x_i)^2 \ll \sigma^2$ for any i. It should be emphasised that we neither impose any "external" a priori constraints to a trend, nor do we assume any definite level of uncertainties in the input data.

3.2.2 Description of the algorithm

The basic steps of our algorithm are the following (see Fig. 5). First, we use use a three-layer feed-forward network with a sigmoid transfer function in combination with a linear regression for approximation of the unknown nonlinear trend:

$$x_{ei}(\mathbf{w}) = \beta_0 + \beta_1 i + \sum_{k=0}^{N} w_{1k} g_k;$$
$$g_k = \frac{1}{1+\exp(w_{2k} i + w_{3k})}, \quad (5)$$

where β_0 and β_1 are coefficients of a linear regression, $\mathbf{w}$ are weight coefficients of a neural network, and N is the number of neurons (see, e.g., Nelson et al., 1991; Bishop, 1995). The linear regression is fitted by the standard least-squares method directly to the input data ($\boldsymbol{y}$), while the neural network is used to approximate only a residual (nonlinear) part in variability of y. By definition, the coefficient w_{10} is set to be zero; that is, if $N=0$, the neural network is not used, and the estimated trend is strictly linear. Neural networks are employed here because they are commonly considered as universal approximators. Specifically, it has been shown (Hornik et al., 1989) that given a sufficient number of neurons, a multi-layer feed-forward network can approximate any smooth function with any given accuracy. Neural networks are extensively used in air pollution studies for approximation of unknown relationships between the observed quantities and forecasting (see, e.g. Gardner and Dorling, 1998; Konovalov 2002, 2003; Lary et al., 2004; Hooyberghs, 2005; Argiriou, 2007; Feister et al., 2008).

Second, we follow the Bayesian probabilistic approach, which is commonly used in inverse modeling and data assimilation studies and is applied here to the estimation of weight coefficients of the neural network. Specifically, using

Bayes's theorem, we get the following a posteriori probability distribution function (*pdf*) for the weight coefficients.

$$p(\mathbf{w}|\boldsymbol{y}) \propto \exp\left[-\sum_{i=1}^{n}\frac{(y_i - x_{ei}(\mathbf{w}))^2}{2\sigma^2}\right] p_a(\mathbf{w}) \quad (6)$$

where $p_a(\mathbf{w})$ is the a priori *pdf*. Here we constrain a priori only the maximum magnitude of the components of $\mathbf{w}$, that is,

$$p_a(\mathbf{w}) = \text{const}(>0) \quad \text{if} \quad |w| < w_{\max};$$
$$p_a(\mathbf{w}) = 0 \quad \text{if} \quad |w| > w_{\max}, \quad (7)$$

where $w_{\max}$ is a parameter estimated as described below, and $|w|$ is the absolute value of any weight coefficient used in the neural network. In other words, the a priori probability of $|w|$ is assumed to be a constant (larger than zero) if $|w|$ is less (or equal) than $w_{\max}$ and zero otherwise. The magnitude of this constant is not important: formally, it can be determined by demanding that the total probability is unity. In principle, we could specify the a priori *pdf* in different ways. The rectangular shape of the a priori *pdf* was chosen as a result of preliminary experiments with both artificial and real data: it was found that this simple structure enables both efficient noise filtering and high sensitivity of the algorithm to actual nonlinearities in input data. The maximum likelihood estimate of $\mathbf{w}$ can then be found as follows:

$$\hat{\mathbf{w}} = \arg\ \min\left[\sum_{i=1}^{n}(y_i - x_{ei})^2\right] | w \in [-w_{\max}; w_{\max}] \quad (8)$$

Third, we use the leave-one-out method of cross validation in order to find the optimal value of $w_{\max}$. The idea is to minimize the difference between a given measurement and an approximation which is built without using this measurement. Specifically, using again Bayes's theorem and assuming a uniform a priori for $w_{\max}$, we obtain the following probability distribution of $w_{\max}$:

$$p(w_{\max}|\boldsymbol{y}) \propto \exp\left[-\sum_{i=1}^{n}\frac{(y_i - x_{ei}(\hat{\mathbf{w}}))^2}{2\sigma^2}\right] \quad (9)$$

The principal point here is that the estimate x_{ei} is obtained without using a corresponding measurement y_i. Based on the third assumption formulated in Sect. 3.2.1, we consider the differences between y_i and x_{ei} as a manifestation of noise. By finding the maximum of this distribution, we estimate $w_{\max}$. If the estimated value of $w_{\max}$ is zero, then it means that either the trend is linear or the nonlinearity is too weak in comparison with the noise level.

In principle, a similar procedure could also be used to optimize the number of neurons, N. However, in practice, it is also necessary to take into account that the uncertainties of estimates x_{ei} obtained with a larger number of neurons are larger. Besides, the differences between estimates obtained with different numbers of neurons are frequently insignificant. Thus we define the optimal number of neurons in a different way. Specifically, we find the estimates of the trends with all values of N in the range from 0 to n/6. The upper limit for N (which is, in our case, equals 2) is determined by the consideration that the number of fitted parameters cannot be larger than a half of the number of data points (taking into account our assumption that each second data point can be regarded as "excessive"). We choose the smallest value of N such that a corresponding nonlinear trend (if it is detected) is significantly different from a linear trend but is not significantly different from trends obtained by the larger numbers of neurons. Evaluation of the statistical significance level (in terms of 68.3 percentile) is based on the uncertainty analysis described below. While minimizing the number of neurons, we also minimize the risk of overfitting. On the other hand, we try to make sure that the network is not underfitted; that is why we test networks with different numbers of neurons. If N optimized in such a way equals zero (this may be, for instance, when $w_{\max} = 0$ for any N considered), the retrieved trend is linear.

Once $w_{\max}$ is optimized, $\boldsymbol{x_e}$ is estimated again, but this time employing the whole time series. Technically, the optimization of $w_{\max}$ is carried out by means of the one-dimensional golden section search method (Press et al., 1992). The optimization of the weight coefficients of the neural network is achieved in the embedded cycle by the Nelder-Mead simplex algorithm (Press et al., 1992).

The noise level is estimated as follows:

$$\sigma^2 \approx \frac{1}{n}\sum\nolimits_{i=1}^{n}(y_i - x_{ei}(\hat{\mathbf{w}}\,|\, w_{\max} = \hat{w}_{\max}))^2. \quad (10)$$

Note that such an estimated noise level takes into account only a random (varying) part of errors in the input data ($\boldsymbol{y}$), assuming that the probability distribution of such errors is stationary. In the case of NO_x emission estimates defined by Eq. (3), σ is determined by uncertainties both in satellite data and model errors. Note also that σ is estimated after having determined the best estimate of weighting coefficients; this estimate does not influence the optimization procedure specified by Eqs. (5)–(9). The estimate of the noise level is further used to assess the uncertainties in results by means of the Monte Carlo method. Specifically, we sample the errors, ε_i, from the normal distribution with σ defined by Eq. (10). Technically, such sampling is performed by means of the Box-Muller method for generating random deviates with a normal distribution (Press et al., 1992). In the problem considered in this study, we have to take into account also the uncertainty of the convolution scale, s_c, and thus we also randomly change this factor within the estimated uncertainty range (see Sect. 2.1). This uncertainty is taken into account even if the algorithm yields only a linear trend. Accordingly, the Monte Carlo experiment consists of the following steps. First, a random perturbation from the lognormal distribution is added to the optimal value of s_c. Second,

the algorithm specified by Eqs. (5)–(9) is applied to the NO_x emission estimates (see Eq. 3) obtained with the perturbed value of s_c. Third, the errors are added to the trend $\boldsymbol{x_e}$ estimated with the perturbed s_c, and the estimation procedure defined by Eqs. (5)–(9) is repeated. These steps are iterated (with the fixed optimal N) many times (in this study, 300). Finally, given a set of samples of $\boldsymbol{x_e}$ generated in the Monte Carlo experiment, we find (by means of a simple iterative procedure) the interval which includes at least 68.3 percent of the samples $\boldsymbol{x_e}$.

Note that the procedure described above enables estimation of only that part of the uncertainties in our results, which are associated with random fluctuations in the input data. Estimation of uncertainties associated with any unidentified drifts in the satellite and model data is much more difficult and goes beyond of the scope of this paper. We expect, however, that the total impact of all potential sources of uncertainties on our estimates can be manifested in the comparison of the retrieved emission trends with independent measurements (see Sect. 4.2).

We characterise trends by the rate of inter-annual changes. Taking into account that the algorithm described above is applied in this study to the log-transformed NO_x emission estimates (see the last paragraph in Sect. 3.1), the relative rate of inter-annual changes, $\boldsymbol{\delta_e}$, is calculated (in percent) as follows:

$$\delta_{ei} = [\exp(x_{i+1} - x_i) - 1] \times 100\,(\%); \quad i = 1, ..., n-1 \quad (11)$$

The uncertainty intervals for the estimated rate of inter-annual changes are derived from the statistical distribution of $\boldsymbol{\delta_e}$ obtained in the Monte-Carlo experiment.

The nonlinearity of the trend is considered as statistically significant if there are at least two different periods such that the corresponding uncertainty intervals of the rates of inter-annual changes do not intersect. In other words, the trend of NO_x emissions is nonlinear if there are statistically significant variations of the rate of emission changes, because a linear trend is characterized by a constant rate.

3.2.3 Testing examples

Before applying it to the real data, the algorithm was tested with artificial time series representing both "ideal" and "noisy" cases. The examples of application of our algorithm to artificial time series are presented in Fig. 6. In both cases, we defined the "true" smooth changes shown in the left plots by red crosses. Similar to the case with real data, the artificial data were log-transformed before application of the trend estimating algorithm. It can be seen that when the noise is absent, the algorithm yields almost ideal fits. Some inaccuracies are the result of constraining the neural network parameters using the cross-validation method. In essence, the uncertainties in the ideal case are due to the sparseness of data points in the time series.

The red crosses in the right plots of Fig. 6 show the data obtained after the noise was added to the same ideal dependencies. The noise level corresponds to that in a real time series of the emission estimates (specifically, for Moscow). It can be seen that in spite of the large noise, our algorithm has managed to retrieve properly at least the qualitative nonlinear features of the "true" variations. Although these tests do not provide a proof of validity of our method, they nevertheless show in an illustrative way that the method is capable to retrieve realistic trend estimates even from very noisy time series.

Table 2. Estimates (*) of the trends in NO_x emission and NO_2 columns for several urban agglomerations (in percent per year).

Cities	NO_x emission trends		Trends in NO_2 columns from satellites
	This study	EMEP	
Bagdad	3.91 (±4.21)	−0.62 (±0.31)	1.59(±0.97)
Barcelona	3.34 (±1.04)	−0.01 (±0.37)	3.05 (±0.78)
Berlin	−5.25 (±1.51)	−3.37 (±0.15)	−3.63 (±0.86)
Istanbul	2.00 (±1.01)	1.72 (±0.40)	1.34 (±0.81)
London	−4.47 (±1.07)	−4.13(±0.27)	−2.86 (±0.89)
Madrid	1.75 (±1.19)	−0.47 (±0.32)	1.77 (±0.95)
Milan	−1.41 (±1.10)	−3.48(±0.19)	0.41 (±0.77)
Moscow	1.88 (±1.62)	3.72(±0.37)	0.50 (±1.61)
Paris	−3.38 (±1.33)	−1.92 (±0.44)	−1.39 (±0.98)
Ruhr region(**)	−4.04 (±1.26)	−4.44 (±0.22)	−1.77 (±0.69)
S.−Petersburg	0.06 (±1.52)	2.65(±0.36)	−0.96 (±1.06)
Tehran	4.47 (±1.50)	−0.63 (±0.51)	3.47 (±1.07)

(*) The reported values represent the relative linear trends (calculated by means of an exponential fit to the data) in average anthropogenic emission rates for three summer months (June to August). The summertime emission estimates based on the EMEP annual data were obtained by means of the CHIMERE emission interface. Values provided in brackets are estimates of uncertainties of the linear fit in terms of the 68.3 percentile. The megacity regions for which the statistically significant differences are found between our estimates and the EMEP inventory are marked in bold. (**) the Ruhr region is defined around the center of Essen.

4 Results

4.1 NO_x emission trend estimates

Our estimates of trends in NO_x emissions in the urban agglomerations considered in this study in comparison with similar trends calculated with the EMEP data are presented in Figs. 7 and 8. Additionally, values of linear trends in our emission estimates in comparison with those derived from the EMEP data are listed in Table 2. Note that the emission data based on the EMEP inventory, which are compared below with the observation based emission trends, represent annual emission data processed by the standard CHIMERE interface to yield the daily average emissions for the summer season only.

Statistically significant nonlinearities are detected in five megacities (Bagdad, Madrid, Milan, Moscow and Paris). Specifically, for Madrid and Moscow we got positive changes in the 1990s and negative changes in more recent

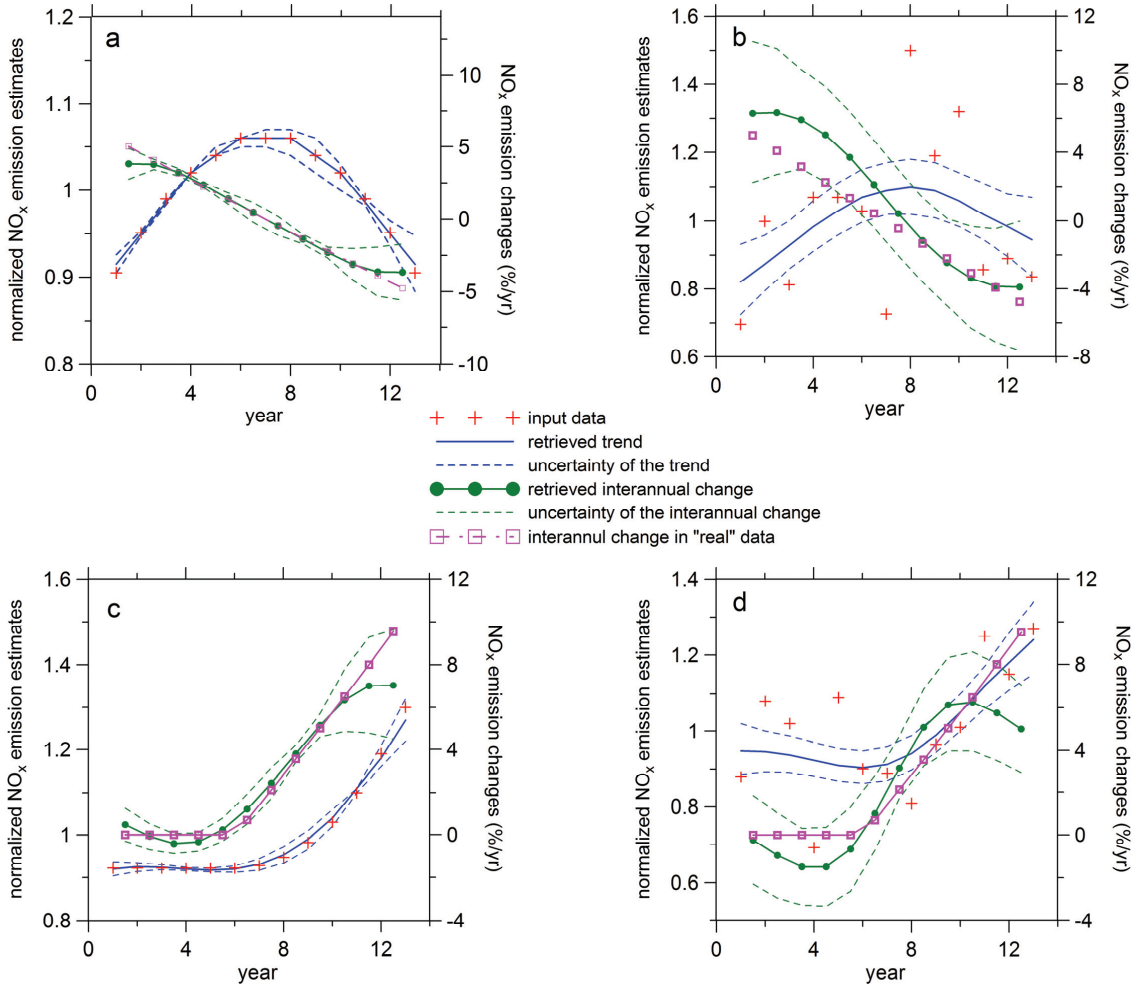

Fig. 6. Examples of application of the nonlinear trend estimation algorithm to artificial time series: **(a, c)** the "ideal" cases where the input data are determined by smooth nonlinear functions and **(b, d)** cases where the input data are determined by the same nonlinear functions but with added random perturbations. The results are obtained with two neurons in the network ($N = 2$). The uncertainties are evaluated in terms of the 68.3 percentile.

years. An interesting nonlinearity which indicates the growth of the rate of the negative trend in recent years is also found for Paris. Most probably, the latest tendencies in Madrid, Moscow, and Paris are related to the increase of the fraction of modern cars equipped with catalytic converters. In contrast, the statistically significant negative trend in Milan in the period from 1996 to 2002 was followed by some increase of emissions (although this increase is not statistically significant). In Bagdad, the statistically significant positive trend is detected since 2003; it can be suggested that this increase of NO_x emissions is associated with economical changes in Iraq triggered by the events of the year 2003.

We would like to emphasize that the trend estimates should be considered together with their uncertainties. Because of the strong noise in input data, we work with a rather low level of statistical significance (0.683): the nonlinearities revealed in this study would not be significant at the 0.90 or 0.95 significance levels. Accordingly, our results should be understood in the probabilistic sense as the most probable (but not necessarily true) estimates derived from the given sets of noisy data under the assumptions specified in the Sect. 3.2.1. However, in most cases some nonlinear tendencies in the input data are visible to naked-eye inspection (see red crosses in Fig. 7); in particular, the most obvious cases are Bagdad and Madrid. Taking this into account, we believe that our estimates are sufficiently meaningful and can be considered by experts together with other relevant data (from, e.g., bottom-up emission inventories).

Nonlinearities are not detected in the other regions, and therefore linear trends are evaluated (see Table 2 and Fig. 8). In particular, strong negative trends are detected in Berlin, London, and the Ruhr agglomeration (-5.2 ± 1.5, -4.5 ± 1.1, -4.0 ± 1.3 percent per year, respectively). In contrast, positive trends are found in Barcelona and Tehran (3.3 ± 1.0 and

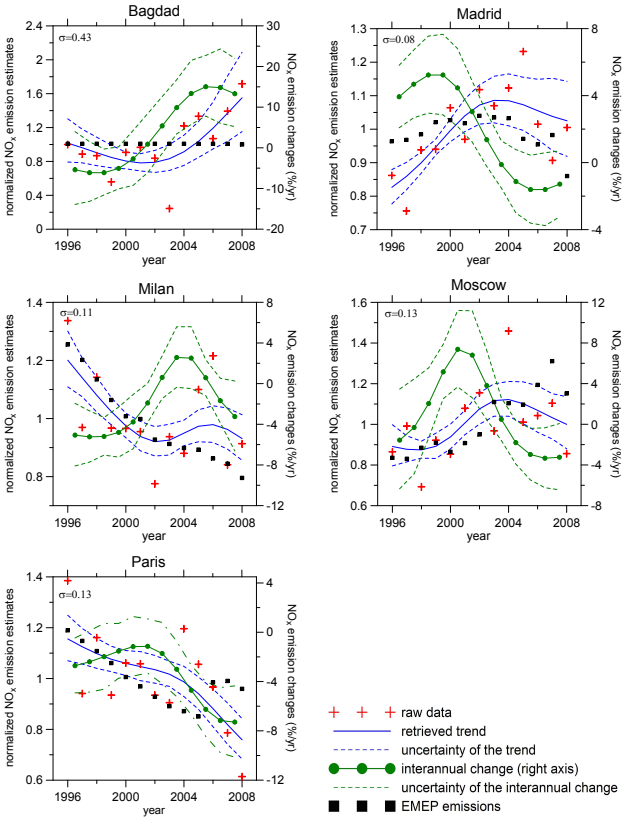

Fig. 7. Trends in NO_X emission estimates retrieved from satellite measurements in comparison with corresponding NO_X emission data derived from the EMEP inventory. The results are obtained with two neurons in the network (N=2). The uncertainties are evaluated in terms of the 68.3 percentile using estimates of the noise level (σ, see Eq. (10)) shown in the plots.

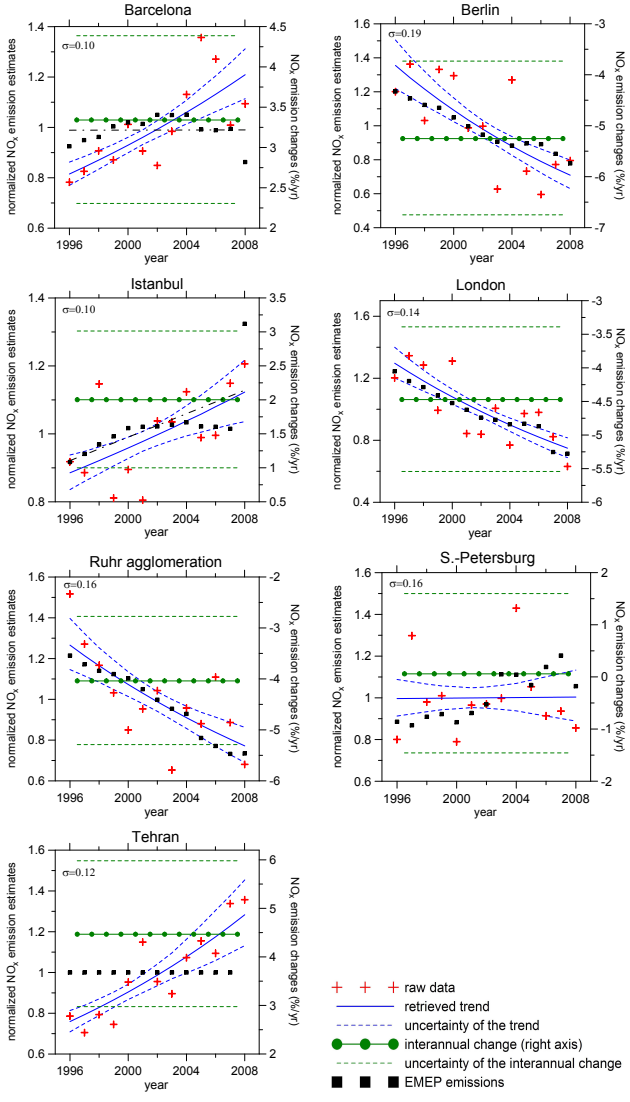

Fig. 8. The same as in Fig. 7 but for the megacity regions where statistically significant nonlinearities in inter-annual emission changes are not detected.

4.5±1.5). Note that a strong positive trend (6.5±1) in NO_2 columns over Tehran in the period from 1996 to 2006 was reported earlier by van der A et al. (2008), based on the analysis of a different product of retrieval of NO_2 columns from the GOME and SCIAMACHY measurements.

The EMEP data are, at least, in qualitative agreement with our estimates in most European megacities (except for Barcelona and S.-Petersburg) and also in Istanbul. Note that the EMEP data for some cities show irregular inter-annual changes which are probably artefacts of changes in methodology used in the EMEP inventory for different years (R. Wankmüller, personal communication, 2009). An example is a "jump" of the EMEP emissions in 2006 in Paris. Changes in the EMEP data for Moscow also do not always look quite realistic; in particular it is difficult to explain why the NO_X emissions slightly decreased between 2004 and 2005 but suddenly strongly increased (by more than 10 percent) between 2005 and 2006. Nonetheless, both the EMEP data and our estimates show strong downward tendencies in Berlin, London, Milan (until 2003), Paris (until 2006), and the Ruhr agglomeration. Both kinds of data also suggest that the NO_X emissions in Moscow during the period from 1996 to 2004 have increased by about 20 percent.

In contrast, our analysis does not confirm the strong decrease of NO_X emissions in Milan and the adjoining urban agglomeration after 2002, as predicted by the EMEP inventory. Our results also suggest that the upward tendencies have been underestimated in the EMEP data for the Spanish cities. Interestingly, the EMEP data for Madrid show, nevertheless, a kind of nonlinearity similar to that revealed in our analysis. The fact that the EMEP data for Bagdad and Tehran are constant indicate that EMEP did not have sufficient information about emissions changes in these megacities, and thus the information provided by satellites is really unique in this case.

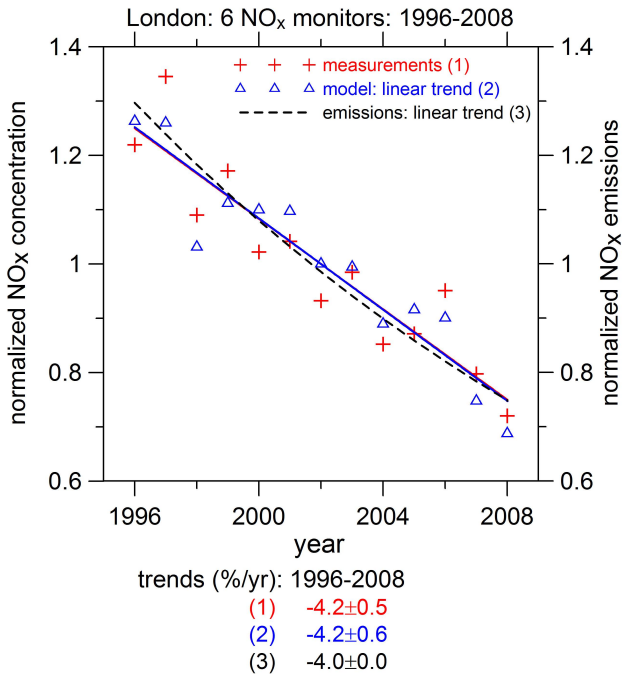

Fig. 9. Comparison of (1) air quality monitoring data in London with (2) simulations based on the relative linear trend in NO_x emissions. The trend estimated as an exponential fit to emission estimates derived from satellite data is also shown (3). The range of uncertainties reported along with values of trends is estimated as the standard deviation of the slope of the linear fit.

Note that if NO_x emission estimates were derived directly from the measured NO_2 columns (as discussed in Sect. 3.1), the linear NO_x emission trends would be statistically different from the linear trends in the EMEP data in London, Moscow and Ruhr agglomeration (see Table 2), while the inverse modeling approach yields no significant differences with the EMEP one for these cities. With the direct approach, the agreement could become significantly better only in the case of Berlin, where our estimates show a stronger negative trend than the EMEP data.

4.2 Validation of derived NO_x emission trend estimates with independent measurements

In this section, we investigate whether the derived NO_x emission trends and their nonlinear features are manifested also in independent surface measurements. We used our estimates of emission trends to scale the base case NO_x emissions in the CHIMERE grid cells attributed to a given agglomeration (see Fig. 1). The model concentrations were compared with the spatial average of the measured concentrations normalized by their temporal average (over all years considered) at each site. The results of the comparison are presented in Figs. 9 and 10.

In the case of London (see Fig. 9), the linear trend in simulated NO_x concentrations coincides with that in the measurements. Although this coincidence is likely occasional, a good agreement between the simulated and measured trends in London was, nevertheless, expected taking into account that the NO_x emission trend in London estimated in this study is very close to that in the EMEP. Also for Great Britain as a whole, changes in NO_x emissions in the EMEP inventory were found to be in accordance to inverted ones in our previous study (Konovalov et al., 2008).

In the case of other cites (see Fig. 10), the quantitative agreement is not as good, but still rather satisfactory, at least in the cases of Paris and Milan. Remaining discrepancies can be explained not only by uncertainties in our emission estimates but also by insufficient spatial coverage of the surface measurements and by model errors. In the context of the given study, it is important to consider if the surface measurements manifest any evidences of nonlinearities in NO_x emission trends. For this purpose, we have performed two model runs based on our estimates of linear and nonlinear trends in NO_x emissions, respectively. The idea of validation of the revealed nonlinearities is to compare linear trends evaluated for two halves of the considered period of the surface measurements and to investigate, whether or not the results from the nonlinear approach agree better with independent observations.

In particular, the linear trends of surface concentrations in Paris are evaluated separately for the periods of 1996–2002 and 2002–2008. The magnitudes of the negative trends in both the measured and simulated concentrations in the second period are much larger than those in the first period. The differences are statistically significant (outside of the total uncertainty range) in both cases. In contrast, the simulations based on the linear estimate of the NO_x emission changes do not demonstrate a statistically significant difference between the two periods. Importantly, there is a quantitative agreement (within the uncertainty range) between the measured and simulated trends in surface concentrations in Paris. Note that, as an additional test, we applied our algorithm directly to surface NO_x observations in Paris. As a result, we found an accelerating negative nonlinear trend, which is in agreement with the trend obtained with satellite data within its uncertainty limits.

The available measurements in the Milan agglomeration show that the linear trend in the period from 1996 to 2003 was significantly different from that in the period from 2003 to 2008: the first period was characterized by a statistically significant negative trend, while the second period shows a positive (although statistically insignificant) trend. Similar features are demonstrated by simulated concentrations obtained with the nonlinear emission trend estimates, except that the trend in the second period is statistically significant. The difference between the trends calculated for the two periods with the linear NO_x emission trend estimates is not statistically significant.

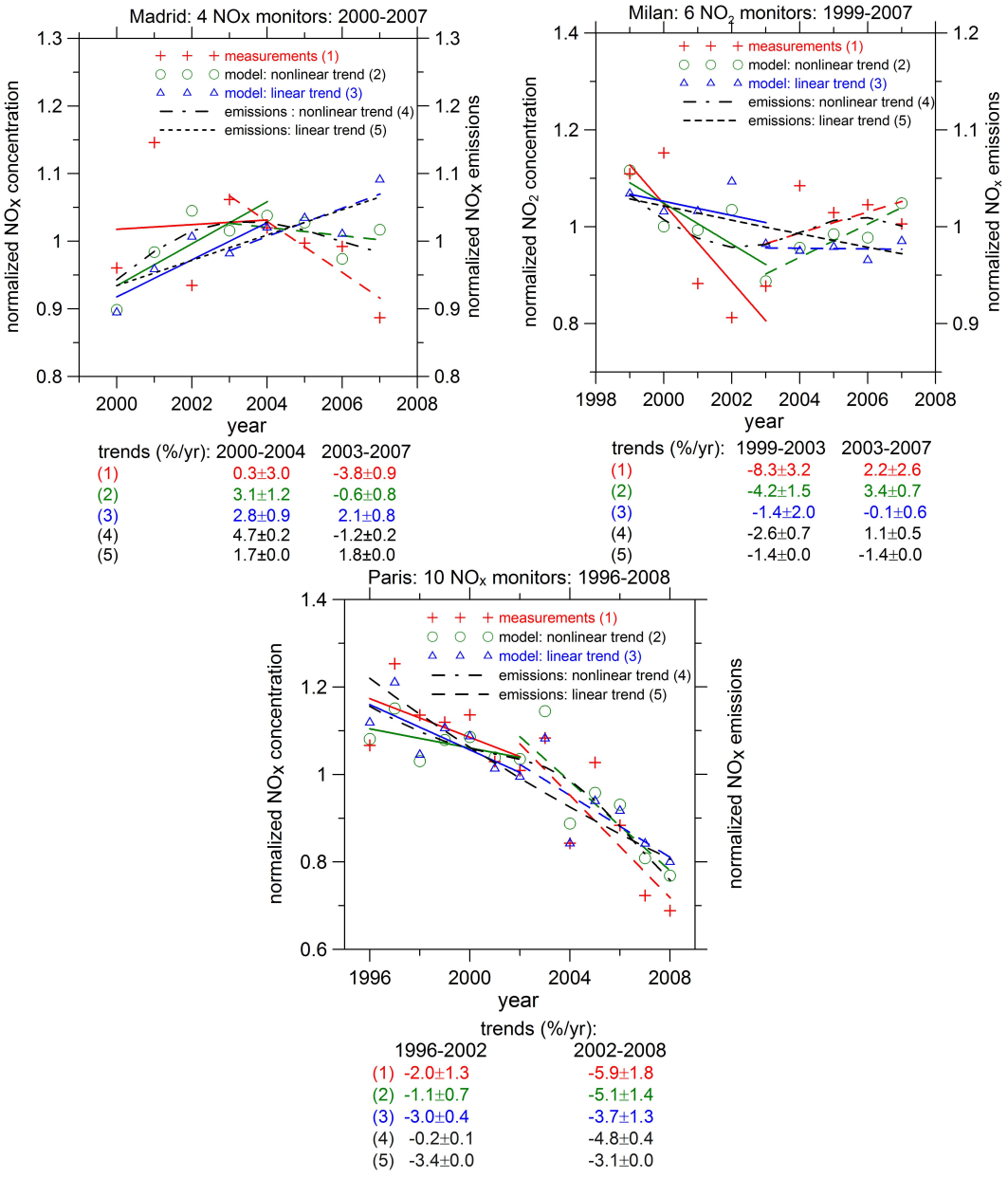

Fig. 10. Comparison of (1) air quality monitoring data with simulations based on (2) nonlinear and (3) linear trends of NO_x emission estimates derived from satellite measurements. The nonlinear (4) and linear (5) NO_x emission trends used in simulations are also shown. The reported uncertainties of the piece-wise linear trends are evaluated as the standard deviation of the slope of the corresponding linear fits.

In the case of Madrid, both simulations based on the nonlinear emission trend estimates and the measurements demonstrate significantly different linear trends for the two (slightly overlapping) periods of 5 years: 2000–2004 and 2003–2007. And again, the nonlinear NO_x emission trend leads to much better agreement of simulations with the measurements than the linear NO_x emission trend. However, there are significant quantitative differences between the trends in the simulated and measured concentrations. These differences could be explained by insufficient spatial representativeness of available surface NO_x measurements in Madrid (because the measurements are mainly performed at traffic sites) and an undetected positive trend (about 3 percent per year) of NO_x emissions from other sources (not apparent at traffic sites).

As a caveat, note that the quantitative results (which are rather encouraging) should be considered with care in view of the limited amount of surface measurement data available for this study and also possible model errors, which may be due, in particular, to insufficient spatial resolution and

possible uncertainties in VOC emission data. As it was already mentioned in Sect. 2, the resolution of the model used in this study was limited not only by consideration of computational costs but also by the resolution of available multi-annual emission data. The difference between the resolution of the EMEP data ($50\times50\,km^2$) and that of our model grid ($1^\circ\times1^\circ$) is small in comparison with the resolution required, ideally, for adequate modeling on urban scales. Indeed, a control multi-annual model run performed with the resolution of $0.5^\circ\times0.5^\circ$ has not revealed any considerable differences in the evolution of NO_x concentrations in comparison with corresponding simulations presented in this paper. Another caveat concerns possible inaccuracies of NO_x measurements performed by chemiluminescence analyzers due to possible interference of non-NO_x reactive nitrogen (NO_z) species (Dunlea et al., 2007). As it is discussed by Konovalov et al. (2008), this interference may lead to some bias of a linear trend in the measured NO_x concentrations, but it is unlikely that such a bias exceeds 10 percent. It seems also very unlikely that the measurement inaccuracies may be responsible for the strong nonlinearities of the trends in NO_x measurement data in Madrid, Milan and Paris, particularly because NO_x at these urban sites is not yet fully oxidized, and thus the measurement inaccuracy is relatively small.

Taking into account all the results presented in this section, we can conclude that surface measurements manifest evidences of nonlinearities in NO_x emission trends, in agreement with the results retrieved from satellite data with our nonlinear trend analysis. Using the results from a linear emission trend analysis leads to poorer agreement between modelled NO_2 and independent measurements.

5 Conclusions

The data for tropospheric NO_2 columns amounts derived from long-term GOME and SCIAMACHY satellite measurements are used to estimate trends in NO_x emissions in the 12 largest urban agglomerations in Europe and the Middle East for a 13 years period (1996–2008). The study is based on the synergetic use of the satellite data and simulations performed with a chemistry transport model. It involves an analysis of different degrees of complexity ranging from evaluation of linear trends in the time series of NO_2 columns derived from satellite measurements to the estimation of nonlinear trends in NO_x emission estimates obtained with an inverse modelling method. The challenging part of the study is the nonlinear trend estimation which is performed by means of an original algorithm enabling filtering out noisy fluctuations caused by measurement and model errors from the retrieved time series of the NO_x emission estimates. The algorithm uses artificial neural networks for fitting the unknown trend and a probabilistic approach along with the cross-validation technique for estimation of its optimal parameters.

It is found that most of the urban agglomerations considered exhibit statistically significant (in terms of 68.3 percentile) linear trends in NO_x emission, ranging from -5.2 (in Berlin) to $+4.5$ (in Tehran) percent per year, with strong negative trends dominating in several Western European agglomerations and positive trends outside of Western Europe. As an exception, positive linear trends are also detected in Spanish cities (in Barcelona and Madrid). This illustrates a general picture of emission control measures having been efficient for most of Western Europe, while increasing urbanization and/or traffic increases emissions especially in Middle-East cities. The agreement between the trends estimated in this study and calculated with the EMEP data is best in London and the Ruhr agglomeration, while the disagreement is strongest in Tehran, where the EMEP data do not exhibit any significant changes.

Statistically significant nonlinearities of NO_x emission trends are revealed in 5 megacity regions (Bagdad, Madrid, Milan, Moscow and Paris). Specifically, for Madrid and Moscow we found positive changes in the 1990s and negative changes in more recent years. An accelerating negative trend was found for Paris. In contrast, the statistically significant negative trend in Milan in the period from 1996 to 2002 is not detected in later years.

Results of model runs using the obtained estimates of emission changes are found to be consistent with independent data of air quality monitoring in London, Milan and Paris. It is found that nonlinear trends are more consistent with near surface measurements than the corresponding linear trends in Madrid (where some quantitative inconsistency was expected because of low spatial representativeness of the available measurements), Milan and Paris. This justifies the attempt to perform a more complex trend analysis including also nonlinear trends.

On the whole, the results of this study confirm that satellite measurements are a source of highly useful information on multi-annual NO_x emission changes, and it demonstrates the feasibility of using a simple inverse modelling method associated with the nonlinear trend analysis for quantifying these changes in megacity regions. This approach may be especially useful for densely populated regions in developing countries where dynamic changes in economic activities may be accompanied by corresponding (nonlinear) variations in air pollutant emissions but where alternative information is insufficient.

Acknowledgements. I. B. Konovalov acknowledges the support by the Russian Foundation for Basic Research (grant No. 08-05-00969) and Russian Academy of Sciences (in the framework of the Programme for Basic Research "Physics of Atmosphere; Electrical Processes, Radiophysical Methods of Research"). The authors acknowledge the support of the European Commission through the FP6 GEOmon Integrated project (the contract number FP6-2005-Global-4-036677) and through the Seventh Framework Programme (FP7/2007-2013) under grant agreement no. 212095 (CITYZEN).

Edited by: P. Middleton

The publication of this article is financed by CNRS-INSU.

References

Argiriou, A. A.: Use of neural networks for tropospheric ozone time series approximation and forecasting – a review, Atmos. Chem. Phys. Discuss., 7, 5739–5767, doi:10.5194/acpd-7-5739-2007, 2007.

Beirle, S., Platt, U., Wenig, M., and Wagner, T.: Weekly cycle of NO_2 by GOME measurements: a signature of anthropogenic sources, Atmos. Chem. Phys., 3, 2225–2232, doi:10.5194/acp-3-2225-2003, 2003.

Beirle, S., Platt, U., Glasow, R. V., Wenig, M., and Wagner T.: Estimate of nitrogen oxide emission from shipping by satellite remote sensing, Geophys. Res. Lett., 31(18), L18102, doi:10.1029/2004GL020312, 2004.

Beirle, S., Spichtinger, N., Stohl, A., Cummins, K. L., Turner, T., Boccippio, D., Cooper, O. R., Wenig, M., Grzegorski, M., Platt, U., and Wagner, T.: Estimating the NO_x produced by lightning from GOME and NLDN data: a case study in the Gulf of Mexico, Atmos. Chem. Phys., 6, 1075–1089, doi:10.5194/acp-6-1075-2006, 2006.

Bertram, T. H., Heckel, A., Richter, A., Burrows, J. P., and Cohen, R. C.: Satellite measurements of daily variations in soil NO_x emissions, Geophys. Res. Lett., 32(24), L24812, doi:10.1029/2005GL024640, 2005.

Bishop, C. M.: Neural Networks for Pattern Recognition, Clarendon Press, Oxford, 504 pp., 1995.

Blond, N., Boersma, K. F., Eskes, H. J., van der A, R. J., Van Roozendael, M., De Smedt, I., Bergametti, G., and Vautard, R.: Intercomparison of SCIAMACHY nitrogen dioxide observations, in situ measurements and air quality modeling results over Western Europe, J. Geophys. Res., 112, D10311, doi:10.1029/2006JD007277, 2007.

Boersma, K. F., Eskes, H. J., Meijer, E. W., and Kelder, H. M.: Estimates of lightning NO_x production from GOME satellite observations, Atmos. Chem. Phys., 5, 2311–2331, doi:10.5194/acp-5-2311-2005, 2005.

Boersma, K. F., Jacob, D. J., Eskes, H. J., Pinder, R. W., Wang, J., and van der A, R. J.: Intercomparison of SCIAMACHY and OMI tropospheric NO_2 columns: Observing the diurnal evolution of chemistry and emissions from space, J. Geophys. Res.-Atmos., 113, D16S26, doi:10.1029/2007JD008816, 2008.

Bovensmann, H., Burrows, J. P., Buchwitz, M., et al.: SCIAMACHY – mission objectives and measurement modes, J. Atmos. Sci., 56, 127–150, 1999.

Brinkhoff, T., The principal agglomerations of the World, availabe online at: http://www.citypopulation.de/world/Agglomerations.html, 2010.

Burrows, J.P., Weber, M., Buchwitz, M., Rozanov, V., Ladstätter-Weißenmayer, A., Richter, A., DeBeek, R., Hoogen, R., Bramstedt, K., Eichmann, K. -U., Eisinger, M., and Perner, D.: The Global Ozone Monitoring Experiment (GOME): Mission concept and first scientific results, J. Atmos. Sci., 56, 151–175, 1999.

Butler, T. M., Lawrence, M. G., Gurjar, B. R., van Aardenne, J., Schultz, M., and Lelieveld, J.: The representation of emissions from megacities in global emission inventories, Atmos. Environ., 42, 703–719, 2008.

Chan, C. K. and Yao, X.: Air pollution in mega cities in China, Atmos. Environ., 42, 1–42, 2008.

Dunlea, E. J., Herndon, S. C., Nelson, D. D., et al.: Evaluation of nitrogen dioxide chemiluminescence monitors in a polluted urban environment, Atmos. Chem. Phys., 7, 2691–2704, doi:10.5194/acp-7-2691-2007, 2007.

Eckhardt, S., Stohl, A., Beirle, S., Spichtinger, N., James, P., Forster, C., Junker, C., Wagner, T., Platt, U., and Jennings, S. G.: The North Atlantic Oscillation controls air pollution transport to the Arctic, Atmos. Chem. Phys., 3, 1769–1778, doi:10.5194/acp-3-1769-2003, 2003.

Enting, I. G.: Inverse problems in atmospheric constituents transport, Cambridge University Press, 464 pp., 2002.

Esposito, M. P., Ferreira, M. L., Sant'Anna, S. M. R., et al.: Relationship between leaf antioxidants and ozone injury in Nicotiana tabacum 'Bel-W3' under environmental conditions in Sao Paulo, SE – Brazil, Atmos. Environ., 43(3), 619–623, 2009.

Feister, U., Junk, J., Woldt, M., Bais, A., Helbig, A., Janouch, M., Josefsson, W., Kazantzidis, A., Lindfors, A., den Outer, P. N., and Slaper, H.: Long-term solar UV radiation reconstructed by ANN modelling with emphasis on spatial characteristics of input data, Atmos. Chem. Phys., 8, 3107–3118, doi:10.5194/acp-8-3107-2008, 2008.

de Foy, B., Lei, W., Zavala, M., Volkamer, R., Samuelsson, J., Mellqvist, J., Galle, B., Martnez, A.-P., Grutter, M., Retama, A., and Molina, L. T.: Modelling constraints on the emission inventory and on vertical dispersion for CO and SO2 in the Mexico City Metropolitan Area using Solar FTIR and zenith sky UV spectroscopy, Atmos. Chem. Phys., 7, 781–801, doi:10.5194/acp-7-781-2007, 2007.

Gardner, M. W. and Dorling, S. R.: Artificial neural networks (the multilayer perceptron) – A review of applications in the atmospheric sciences, Atmos. Environ., 32, 2627–2636, 1998.

Hauglustaine, D. A., Hourdin, F., Jourdain, L., Filiberti, M.-A., Walters, S., Lamarque, J.-F., and Holland, E. A.: Interactive chemistry in the Laboratoire de Meteorologie Dynamique general circulation model: Description and background tropospheric chemistry evaluation, J. Geophys. Res., 109, D04314, doi:10.1029/2003JD003, 2004.

Hornik, K., Stinchcombe, M., and White, H.: Multilayer feedforward networks are universal approximators, Neural Networks, 2, 359–366, 1989.

Hooyberghs, J., Mensink, C., Dumont, G., Fierens, F., and Brasseur, O.: A neural network forecast for daily average PM_{10} concentrations in Belgium, Atmos. Environ., 39, 3279–3289, 2005.

Jaeglé, L., Martin, R. V., Chance, K., Steinberger, L., Kurosu, T. P., Jacob, D. J., Modi, A.I., Yoboué, V., Sigha-Nkamdjou, L., and Galy-Lacaux, C.: Satellite mapping of rain-induced nitric oxide emissions from soils, J. Geophys. Res., 109, D21310, doi:10.1029/2004JD004787, 2004.

Kaynak, B., Hu, Y., Martin, R. V., Sioris, C. E., and Russell, A. G., Comparison of weekly cycle of NO_2 satellite retrievals and NO_x emission inventories for the continental US, J. Geophys. Res., 114, D05302, doi:10.1029/2008JD010714, 2009.

Kim, S.-W., Heckel, A., McKeen, S. A., Frost, G. J., Hsie, E.-Y., Trainer, M. K., Richter, A., Burrows, J. P., Peckham, S. E., and Grell, G. A.: Satellite-observed US power plant NO_x emission reductions and their impact on air quality, Geophys. Res. Lett., 33, L22812, doi:10.1029/2006GL027749, 2006.

Kim, S.-W., Heckel, A., Frost, G. J., Richter, A., Gleason, J., Burrows, J. P., McKeen, S., Hsie, E.-Y., Granier, C., and Trainer, M.: NO_2 columns in the western United States observed from space and simulated by a regional chemistry model and their implications for NO_x emissions, J. Geophys. Res., 114, D11301, doi:10.1029/2008JD011343, 2009.

Konovalov, I. B.: Application of neural networks for studying nonlinear relationships between ozone and its precursors, J. Geophys. Res.-Atmos., 107, 4122, doi:10.1029/2001JD000863, 2002.

Konovalov, I. B.: Nonlinear relationships between atmospheric aerosol and its gaseous precursors: Analysis of long-term air quality monitoring data by means of neural networks, Atmos. Chem. Phys., 3, 607–621, doi:10.5194/acp-3-607-2003, 2003.

Konovalov, I. B., Beekmann, M., Vautard, R., Burrows, J. P., Richter, A., Nüß, H., and Elansky, N.: Comparison and evaluation of modelled and GOME measurement derived tropospheric NO_2 columns over Western and Eastern Europe, Atmos. Chem. Phys., 5, 169–190, doi:10.5194/acp-5-169-2005, 2005.

Konovalov, I. B., Beekmann, M., Richter, A., and Burrows, J. P.: Inverse modelling of the spatial distribution of NO_x emissions on a continental scale using satellite data, Atmos. Chem. Phys., 6, 1747–1770, doi:10.5194/acp-6-1747-2006, 2006a.

Konovalov, I. B., Beekmann, M., Richter, A., and Burrows, J. P.: The use of satellite and ground based measurements for estimating and reducing uncertainties in the spatial distribution of emissions of nitrogen oxides, arXiv: physics/0612144 (www.arxiv.org), 2006b.

Konovalov I. B.: Regional differences in decadal changes of the atmospheric emissions of nitrogen oxides in the European part of Russia: results of the inverse modeling based on satellite measurements, Dokl. Earth Sci., 417(5), 685–688, 2007.

Konovalov, I. B., Beekmann, M., Burrows, J. P., and Richter, A.: Satellite measurement based estimates of decadal changes in European nitrogen oxides emissions, Atmos. Chem. Phys., 8, 2623–2641, doi:10.5194/acp-8-2623-2008, 2008.

Kurokawa, J., Yumimoto, K., Uno, I., and Ohara, T.: Adjoint inverse modeling of NO_x emissions over eastern China using satellite observations of NO_2 vertical column densities, Atmos. Environ., 43, 1878–1887, 209.

Lary, D. J., Müller, M. D., and Mussa, H. Y.: Using neural networks to describe tracer correlations, Atmos. Chem. Phys., 4, 143–146, doi:10.5194/acp-4-143-2004, 2004.

Lawrence, M. G., Butler, T. M., Steinkamp, J., Gurjar, B. R., and Lelieveld, J.: Regional pollution potentials of megacities and other major population centers, Atmos. Chem. Phys., 7, 3969–3987, doi:10.5194/acp-7-3969-2007, 2007.

Lei, W., Zavala, M., de Foy, B., Volkamer, R., and Molina, L. T.: Characterizing ozone production and response under different meteorological conditions in Mexico City, Atmos. Chem. Phys., 8, 7571–7581, doi:10.5194/acp-8-7571-2008, 2008.

Lin, J.-T., McElroy, M. B., and Boersma, K. F.: Constraint of anthropogenic NO_x emissions in China from different sectors: a new methodology using multiple satellite retrievals, Atmos. Chem. Phys., 10, 63–78, doi:10.5194/acp-10-63-2010, 2010.

Marshall, J.: Megacity, mega mess ..., Nature, 437(7057), 312–314, 2005.

Martin, R. V., Jacob, D. J., Chance, K., Kurosu, T., Palmer, P. I., and Evans, M. J.: Global inventory of nitrogen oxide emissions constrained by space-based observations of NO_2 columns, J. Geophys. Res., 108, 4537, doi:10.1029/2003JD003453, 2003.

Martin, R. V., Sioris, C. E., Chance, K., Ryerson, T. B., Bertram, T. H., Wooldridge, P. J., Cohen, R. C., Neuman, J. A., Swanson, A., and Flocke, F. M.: Evaluation of space-based constraints on global nitrogen oxide emissions with regional aircraft measurements over and downwind of eastern North America, J. Geophys. Res., 111, D15308, doi:10.1029/2005JD006680, 2006.

Martin, R. V., Sauvage, B., Folkins, I., Sioris, C. E., Boone, C., Bernath, P., and Ziemke, J.: Space-based constraints on the production of nitric oxide by lightning, J. Geophys. Res., 112, D09309, doi:10.1029/2006JD007831, 2007.

Meinardi, S., Nissenson, P., Barletta, B, Dabdub, D., Rowland, F. S, and Blake, D. R.: Influence of the public transportation system on the air quality of a major urban center. A case study: Milan, Italy, Atmos. Environ., 42(34), 7915–7923, 2008.

Miyakawa, T., Takegawa, N., and Kondo, Y.: Photochemical evolution of submicron aerosol chemical composition in the Tokyo megacity region in summer, J. Geophys. Res., 113, D14304, doi:10.1029/2007JD009493, 2008.

Molina, M. J. and Molina, L. T.: Megacities and atmospheric pollution, J. Air Waste Manage. Assoc., 54, 644–680, 2004.

Molina, L. T., Kolb, C. E., de Foy, B., Lamb, B. K., Brune, W. H., Jimenez, J. L., Ramos-Villegas, R., Sarmiento, J., Paramo-Figueroa, V. H., Cardenas, B., Gutierrez-Avedoy, V., and Molina, M. J.: Air quality in North America's most populous city – overview of the MCMA-2003 campaign, Atmos. Chem. Phys., 7, 2447–2473, doi:10.5194/acp-7-2447-2007, 2007.

Moore, J. C., Grinsted, A., and Jevrejeva, S.: New tools for analyzing time series relationships and trends, EOS, Trans. Am. Geophys. Union, 86, 226–232, 2005.

Napelenok, S. L., Pinder, R. W., Gilliland, A. B., and Martin, R. V.: A method for evaluating spatially-resolved NO_x emissions using Kalman filter inversion, direct sensitivities, and space-based NO_2 observations, Atmos. Chem. Phys., 8, 5603–5614, doi:10.5194/acp-8-5603-2008, 2008.

Nelson, M. C. and Illingworth, W. T.: A Practical Guide to Neural Nets, Reading, MA, USA, Addison-Wesley, 1991.

Nunnermacker, L. J., Weinstein-Lloyd, J. B., Hillery, B., Giebel, B., Kleinman, L. I., Springston, S. R., Daum, P. H., Gaffney, J., Marley, N., and Huey, G.: Aircraft and ground-based measurements of hydroperoxides during the 2006 MILAGRO field campaign, Atmos. Chem. Phys., 8, 7619–7636, doi:10.5194/acp-8-7619-2008, 2008.

Press, W. H., Teukolsky, S. A., Vetterling, W. T., and Flannery, B. P.: Numerical Recipes, 2nd edition, Cambridge University Press, 973 pp., 1992.

Reinsel, G. C., Miller, A. J., Weatherhead, E. C., Flynn, L. E., Nagatani, R. M., Tiao, and G. C., and Wuebbles, D. J.: Trend analysis of the ozone data for turnaround and dynamical contributions,

J. Geophys. Res., 110, D16306, doi:10.1029/2004JD004662.

Richter, A., Eyring, V., Burrows, J. P., Bovensmann, H., Lauer, A. Sierk, B., and Crutzen, P. J.: Satellite Measurements of NO2 from International Shipping Emissions, Geophys. Res. Lett., 31, L23110, doi:10.1029/2004GL020822, 2004.

Richter, A., Burrows, J. P., Nüß, H., Granier, C., and Niemeier, U.: Increase in Tropospheric Nitrogen Dioxide Over China Observed from Space, Nature, 437, 129–132, doi:10.1038/nature04092, 2005.

Singh, H. B., Brune, W. H., Crawford, J. H., Flocke, F., and Jacob, D. J.: Chemistry and transport of pollution over the Gulf of Mexico and the Pacific: spring 2006 INTEX-B campaign overview and first results, Atmos. Chem. Phys., 9, 2301–2318, doi:10.5194/acp-9-2301-2009, 2009.

Stavrakou, T., Muller, J. F., Boersma, K. F., De Smedt, I., and van der A, R. J.: Assessing the distribution and growth rates of NO_x emission sources by inverting a 10-year record of NO_2 satellite columns, Geophys. Res. Lett., 35(10), L10801, doi:10.1029/2008GL033521, 2008.

Toenges-Schuller, N., Stein, O., Rohrer, F., Wahner, A., Richter, A., Burrows, J. P., Beirle, S., Wagner, T., Platt, U., and Elvidge, C. D.: Global distribution pattern of anthropogenic nitrogen oxide emissions: Correlation analysis of satellite measurements and model calculations, J. Geophys. Res., 111, D05312, doi:10.1029/2005JD006068, 2006.

UNECE: Present state of emission data, ECE/EB.AIR/97, 2009.

Uno, I., He, Y., Ohara, T., Yamaji, K., Kurokawa, J.-I., Katayama, M., Wang, Z., Noguchi, K., Hayashida, S., Richter, A., and Burrows, J. P.: Systematic analysis of interannual and seasonal variations of model-simulated tropospheric NO_2 in Asia and comparison with GOME-satellite data, Atmos. Chem. Phys., 7, 1671–1681, doi:10.5194/acp-7-1671-2007, 2007.

van der A, R. J. M, Peters, D. H. M. U., Eskes, H., Boersma, K. F., Van Roozendael M., De Smedt, I., and Kelder, H. M.: Detection of the trend and seasonal variation in tropospheric NO_2 over China, J. Geophys. Res., 111, D12317, doi:10.1029/2005JD006594, 2006.

van der A, R. J., Eskes, H. J., Boersma, K. F., van Noije, T. P. C., Van Roozendael M., De Smedt, I., Peters, H. M. U. D., and Meijer E. W.: Trends, seasonal variability and dominant NO_x source derived from a ten year record of NO_2 measured from space, J. Geophys. Res., 113, D04302, doi:10.1029/2007JD009021, 2008.

Vestreng, V., Ntziachristos, L., Semb, A., Reis, S., Isaksen, I. S. A., and Tarrasón, L.: Evolution of NO_x emissions in Europe with focus on road transport control measures, Atmos. Chem. Phys., 9, 1503–1520, doi:10.5194/acp-9-1503-2009, 2009.

Vyushin, D. I., Fioletov, V. E., and Shepherd, T. G.: Impact of long-range correlations on trend detection in total ozone, J. Geophys. Res., 112, D14307, doi:10.1029/2006JD008168, 2007.

Wang, T., Ding, A. J., Gao, J., and Wu, W. S.: Strong ozone production in urban plumes from Beijing, China, Geophys. Res. Lett., 33, L21806, doi:10.1029/2006GL027689, 2006.

Wang, Y., McElroy, M. B., Martin, R. V., Streets, D. G., Zhang, Q., and Fu, T.-M.: Seasonal variability of NO_x emissions over east China constrained by satellite observations: Implications for combustion and microbial sources, J. Geophys. Res., 112, D06301, doi:10.1029/2006JD007538, 2007.